

Influence of the distribution of magnetic moments on the magnetization and magnetoresistance in granular alloys

E. F. Ferrari, F. C. S. da Silva, and M. Knobel

Instituto de Física "Gleb Wataghin" Universidade Estadual de Campinas (UNICAMP),

CP 6165, 13083-970, Campinas, São Paulo, Brazil

(Received 6 May 1997)

In granular solids, the magnetoresistance is directly related to the macroscopic magnetization, but this relationship is extremely complex due to the distribution of grain sizes and the intergranular magnetic interactions. The dependence of the magnetoresistance on the magnetization is here investigated by means of a theoretical model that is developed taking explicitly into account the magnetic moment distribution and the spin-dependent electron-impurity scattering within magnetic grains and at the interface between the grains and the metallic matrix. Using this model, one can explain large experimental deviations from the parabolic behavior of the magnetoresistance vs magnetization curves that are typically expected for equal noninteracting superparamagnetic grains. The expressions for the magnetization and magnetoresistance, obtained for general distribution functions, are tested considering a log-normal-type distribution function by fitting on data obtained from melt-spun $\text{Cu}_{90}\text{Co}_{10}$ ribbons after annealing by dc Joule heating. The experimental data are well traced using just three parameters that determine the particle size distribution, the particle density, and the ratio of the scattering cross section at the boundaries of the grains to the scattering cross section within the grains. [S0163-1829(97)06134-1]

I. INTRODUCTION

Since the discovery of giant magnetoresistance (GMR) in granular solids,^{1,2} it was established that the best representation of the resistance data must be as a function of the material magnetization, and not as a function of the applied field. In fact, magnetoresistance data displaying large hysteresis when represented against the applied field seem to lie in a single curve that resembles an inverted parabola when plotted as a function of the relative magnetization M/M_s . Indeed, using simple arguments about a random distribution of noninteracting magnetic moments of the same magnitude, one easily arrives at the result that the magnetoresistance ratio must display a quadratic dependence on the relative magnetization.³ However, numerous research groups have found that the quadratic law was not followed in several granular systems. Some experimental results were shown to follow a parabola in the low-field region, but a discrepancy appeared when $M/M_s \approx 1$.^{2,4} Other results followed a parabolic law in the high-field region, but a clear deviation from a parabola was evidenced at $M/M_s \approx 0$ (flat-top parabola).⁵ A wide variety of arguments have been employed to explain the deviations from the expected quadratic behavior of an assembly of superparamagnetic particles, some taking into account magnetic interactions, others considering some specific particle distributions or even the presence of different magnetic phases.⁶⁻¹² There are discrepancies concerning the region where the main alteration of the form of the GMR vs M/M_s curve occurs,^{2,5,10,13} and the existing models are still far from a complete explanation of the observed phenomena.

As a matter of fact, the vast diversity of theoretical and experimental results concerning the dependence of the magnetoresistance on magnetization indicates that, if properly understood, this kind of plot can reveal important informa-

tion about the basic mechanisms of spin-dependent transport in granular solids. However, due to the inherent complexity of these systems, this goal must be achieved in a step-by-step procedure. The first approach to the problem, which we will deal with in this work, is to consider that the system is composed only of superparamagnetic particles, without taking into account the magnetic interactions that may be present, neither of dipolar nor RKKY origin. In the model, we develop in further detail some ideas expressed by Zhang and Levy.⁶ We introduce the magnetic moment distribution function and the effect on magnetoresistance of the selective electronic scattering within the magnetic grains and at the magnetic-nonmagnetic interface. From the general expressions of the magnetization and magnetoresistance, we obtain, in the low- and high-field limits, the magnetoresistance as a function of the relative magnetization and calculate the parameters that characterize the flatness of the normalized GMR vs M/M_s curve relative to the square parabola.

The theoretical model is tested for heat-treated Cu-Co melt-spun ribbons, using a log-normal-type distribution function. The magnetization curves are fitted using two parameters, the mean magnetic moment and the geometric standard deviation of the distribution function. Only one additional parameter is necessary to fit the magnetoresistance curves, and it gives an estimate of the relative importance of boundary to bulk scattering in the giant magnetoresistance phenomenon. Some experimental data displaying a distorted parabola are very well described using this model, indicating that the distribution of magnetic moments (or particle volumes) has a strong influence on the magnetotransport behavior. However, there is a theoretical limit up to which the distribution of grain sizes can explain the flatness of the observed curves, and beyond this limit it is not possible to explain the data using a simple superparamagnetic model. In

this case, magnetic interactions must be introduced, consisting of a natural development of the model that will be considered in future works. For the moment, one can already extract important information from the magnetization and magnetoresistance curves, including the particle size distribution and the degree of predominance of interface scattering over the scattering inside the magnetic grains. From these results, one can affirm that the distribution of magnetic moments must always be taken into account in theories that describe the magnetoresistance in granular solids, although introducing further complexity into the already complicated mechanisms that give rise to GMR in these systems.

II. THEORETICAL MODEL

A. Magnetization

Let $f(\mu)$ be the distribution function of magnetic moments in a system of superparamagnetic grains. The number of grains per unit volume of the sample with magnetic moment between μ and $\mu + d\mu$ is given by $f(\mu)d\mu$.

The magnetization of a system of superparamagnetic grains in the magnetic field H is described by

$$M(H, T) = \int_0^\infty \mu L\left(\frac{\mu H}{kT}\right) f(\mu) d\mu, \quad (1)$$

where $L(\mu H/kT)$ is the Langevin function:

$$L\left(\frac{\mu H}{kT}\right) = \coth\left(\frac{\mu H}{kT}\right) - \frac{kT}{\mu H}. \quad (2)$$

The saturation magnetization is given by

$$M_s = \int_0^\infty \mu f(\mu) d\mu = N \langle \mu \rangle, \quad (3)$$

where $\langle \mu \rangle$ is the mean magnetic moment per grain and N is the number of grains per unit volume of the sample,

$$N = \int_0^\infty f(\mu) d\mu. \quad (4)$$

At this initial point, we would like to stress the difference between $f(\mu)$ and the particle volume distribution function $f(v)$ usually introduced by means of the definition of the relative magnetization, namely,

$$\frac{M}{M_s} = \int_0^\infty L\left(\frac{I_s v H}{kT}\right) f(v) dv, \quad (5)$$

where I_s is the grain magnetization, $I_s = \mu/v$.

From Eqs. (1) and (5), we obtain the following relationship between the distribution functions:

$$f(v) dv = \frac{\mu}{M_s} f(\mu) d\mu. \quad (6)$$

Therefore, $f(v)dv$ is not obtained from $f(\mu)d\mu$ through a change of variables like $\mu = I_s v$ and should not be simply interpreted as the density of particles with volume between v and $v + dv$, but as the relative contribution from particles of volume v and magnetic moment μ to the saturation magnetization. Generally speaking, one does not encounter a

clear distinction between both distribution functions in the literature and sometimes their meanings are confused, which may be the cause of rough misinterpretations.

B. Magnetoresistance

The giant magnetoresistance in granular systems is an additional resistance due to electron scattering from nonaligned magnetic grains.^{4,14} The experimental setup is quite simple, and the electrical resistance R is measured as a function of the applied field H in a fixed temperature T . The magnetoresistance ratio is usually defined by

$$\text{MR}(H, T) = \frac{R(H, T) - R(0, T)}{R(0, T)}. \quad (7)$$

It is well established that the basic mechanism giving rise to GMR is the spin-dependent scattering within the magnetic grains and at the interface between the magnetic grains and the metallic matrix. Extensive experimental data have shown that the scattering at the interface predominates over the scattering within the grain.^{1,6,15,16} A simple relationship between the GMR ratio and the magnetization can be found if one considers a system of noninteracting superparamagnetic particles. In this way, assuming that (i) the grains have the same size and (ii) the field-dependent part of electron scattering is proportional to the degree of correlation of the moments of neighboring grains averaged over all configurations, the magnetoresistance results in being proportional to the square of the magnetization, $\text{MR} \propto -(M/M_s)^2$ (Ref. 3).

In order to introduce the distribution of magnetic moments, we start with the model proposed by Zhang and Levy,⁶ in which an expression for the magnetoresistance is derived using the formalism developed for layered structures with currents perpendicular to the plane of the layers, and so we also take into account both scattering mechanisms that contribute to the magnetoresistance. From Eqs. (6), (7), and (11) of Ref. 6, we obtain the magnetoresistance in the following form:

$$\text{MR}(H, T) = -\frac{A}{N^2} \left[\int_0^\infty (\mu + \alpha \mu^{2/3}) L\left(\frac{\mu H}{kT}\right) f(\mu) d\mu \right]^2, \quad (8)$$

where A and α are proportionality coefficients that do not depend on H .

Both scattering mechanisms contribute to the magnetoresistance expression by means of the factor $\mu + \alpha \mu^{2/3}$. The parameter α is directly proportional to the ratio between the interface and bulk scattering cross sections and is given by

$$\alpha = a_0 (36\pi)^{1/3} \frac{p_s \lambda_m}{p_b \lambda_s} I_s^{1/3}, \quad (9)$$

where a_0 is the lattice constant of the grains, p_s and p_b are the ratios of the spin-dependent potentials to the spin-independent potentials, and λ_s and λ_m are the mean free paths that characterize interface roughness and impurity scattering in grains.⁶

The saturation magnetoresistance is given by

$$\text{MR}_s = -A (\langle \mu \rangle + \alpha \langle \mu^{2/3} \rangle)^2, \quad (10)$$

where for any number q the mean value of μ^q is defined by

$$\langle \mu^q \rangle = \frac{1}{N} \int_0^\infty \mu^q f(\mu) d\mu. \quad (11)$$

In the next section, we will apply Eqs. (1) and (8) to experimental data obtained from $\text{Cu}_{90}\text{Co}_{10}$ ribbons. Then, it will be clear that $\alpha \approx 10\langle \mu \rangle^{1/3}$, a result that supports the proposed mechanisms about the origin of giant magnetoresistance. Our simulations reveal that if we neglect the factor $\mu + \alpha\mu^{2/3}$, we cannot trace the experimental data with Eqs. (1) and (8) using the same distribution function. Also, if one neglects scattering within the grains and retains only the contribution from scattering at the interface, i.e., if one assumes that $\alpha\mu^{2/3} \gg \mu$, then once more Eqs. (1) and (8) cannot be fitted on experimental data with the same distribution function. In fact, the calculation of particle sizes from magnetization and magnetoresistance curves was done by von Helmholt *et al.* under a similar assumption (i.e., neglecting the scattering within the magnetic grains) and they obtained a difference between the calculated mean particle radii ($r_{\text{mag}} = 1.2$ nm from the magnetization curve and $r_{\text{res}} = 1.0$ nm from the magnetoresistance curve) that corresponds to a large difference of 73% between the mean magnetic moments.¹⁷ By introducing the factor $\mu + \alpha\mu^{2/3}$, no such difference appears between the distribution functions, and the parameter α can be evaluated as a measure of the predominance of scattering at the interface over scattering within the grains.

C. Magnetoresistance vs magnetization

In order to compare the GMR vs M/M_s curve with the parabola expected for an assembly of noninteracting superparamagnetic particles of the same size, let us now determine the relationship between magnetization and magnetoresistance in the two limiting cases when the magnetic field is small and when the magnetic field is high. For small fields, $\mu H/kT \ll 1$ and thus $L(\mu H/kT) \approx \mu H/3kT$. Consequently, Eqs. (1) and (8) reduce to

$$M = \frac{H}{3kT} N \langle \mu^2 \rangle \quad (12)$$

and

$$\text{MR} = -A \left(\frac{H}{3kT} \langle \mu^2 \rangle \right)^2 \left(1 + \alpha \frac{\langle \mu^{5/3} \rangle}{\langle \mu^2 \rangle} \right)^2. \quad (13)$$

Taking into account Eqs. (3), (12), and (13), we obtain a quadratic dependence of magnetoresistance on magnetization:

$$\text{MR} = -A \langle \mu \rangle^2 \left(1 + \alpha \frac{\langle \mu^{5/3} \rangle}{\langle \mu^2 \rangle} \right)^2 \left(\frac{M}{M_s} \right)^2. \quad (14)$$

For high fields, $\mu H/kT \gg 1$ and therefore $L(\mu H/kT) \approx 1 - kT/\mu H$. In this case, Eqs. (1) and (8) acquire the following forms:

$$M = N \langle \mu \rangle \left(1 - \frac{kT}{\langle \mu \rangle H} \right) \quad (15)$$

and

$$\begin{aligned} \text{MR} = & -A \langle \mu \rangle^2 \left(1 + \alpha \frac{\langle \mu^{2/3} \rangle}{\langle \mu \rangle} \right)^2 \\ & \times \left(1 - \frac{kT}{\langle \mu \rangle H} \frac{1 + \alpha \langle \mu^{-1/3} \rangle}{1 + \alpha \langle \mu^{2/3} \rangle / \langle \mu \rangle} \right)^2. \end{aligned} \quad (16)$$

Taking into account Eqs. (3), (15), and (16), we express the dependence of magnetoresistance on magnetization in the following form:

$$\text{MR} = -A \langle \mu \rangle^2 \left(1 + \alpha \frac{\langle \mu^{2/3} \rangle}{\langle \mu \rangle} \right)^2 \left[1 - f \left(1 - \frac{M}{M_s} \right) \right]^2, \quad (17)$$

where the factor f is defined by

$$f = \frac{1 + \alpha \langle \mu^{-1/3} \rangle}{1 + \alpha \langle \mu^{2/3} \rangle / \langle \mu \rangle}. \quad (18)$$

When the magnetic moment distribution is narrow [in the limit, $f(\mu) = N \delta(\mu - \langle \mu \rangle)$], both Eqs. (14) and (17) have the same parabolic form, namely,

$$\text{MR} = -A (\langle \mu \rangle + \alpha \langle \mu \rangle^{2/3})^2 \left(\frac{M}{M_s} \right)^2. \quad (19)$$

However, when the distribution is broad, Eq. (17) differs from Eq. (14) in the dependence on the relative magnetization and also in the proportionality factor, and for high fields the magnetoresistance curve is not any more a parabola, but tends to a straight line with the slope $2f \times \text{MR}_s$.

Summarizing, we express the normalized magnetoresistance (ranging from -1 to 0) as

$$\text{MR}_n = -\frac{\text{MR}}{\text{MR}_s} = \begin{cases} -g^2 \left(\frac{M}{M_s} \right)^2 & \left(\frac{\mu H}{kT} \ll 1 \right), \\ -\left[1 - f \left(1 - \frac{M}{M_s} \right) \right]^2 & \left(\frac{\mu H}{kT} \gg 1 \right), \end{cases} \quad (20)$$

where the factor g is defined by

$$g = \frac{1 + \alpha \langle \mu^{5/3} \rangle / \langle \mu^2 \rangle}{1 + \alpha \langle \mu^{2/3} \rangle / \langle \mu \rangle}. \quad (21)$$

We can easily show that, for any magnetic moment distribution and for any value of $\alpha > 0$, the characteristic parameters f and g satisfy the following conditions:

$$1 \leq f \leq \frac{\langle \mu^{-1/3} \rangle \langle \mu \rangle}{\langle \mu^{2/3} \rangle}, \quad \frac{\langle \mu^{5/3} \rangle \langle \mu \rangle}{\langle \mu^2 \rangle \langle \mu^{2/3} \rangle} \leq g \leq 1. \quad (22)$$

Owing to these conditions, the MR_n vs M/M_s curve results in being a broad parabola in the low-magnetic-field region (due to the fact that $g < 1$), but saturates slower than a square parabola when the field is high (since $f > 1$) [see Fig. 1(a)].

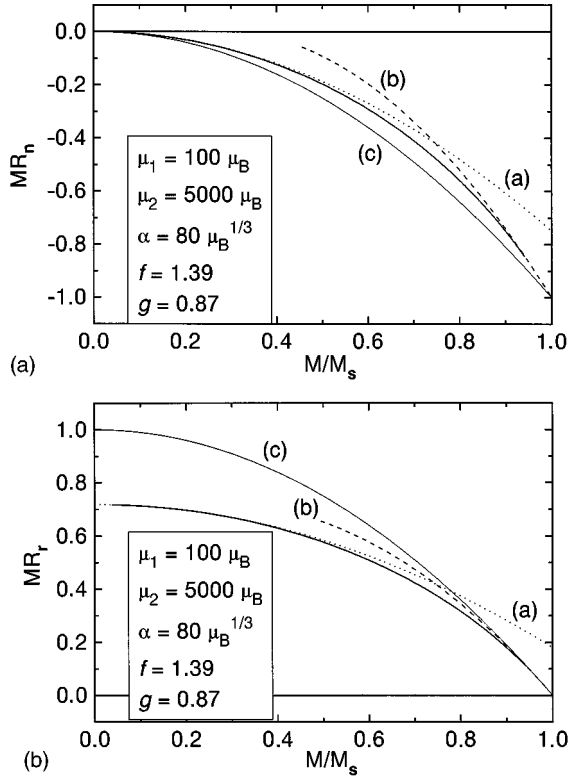


FIG. 1. (a) Normalized magnetoresistance vs relative magnetization curve calculated for a boxlike distribution function with $\mu_1 = 100\mu_B$, $\mu_2 = 5000\mu_B$, and $\alpha = 80\mu_B^{1/3}$ (dots). Curve (a) was calculated in the low-field limit and curve (b) in the high-field limit; the normalized parabola (c) was drawn for comparison. (b) Reduced magnetoresistance vs relative magnetization curve calculated with the same parameters. The flatness of both magnetoresistance curves is characterized by the parameters $f = 1.39$ and $g = 0.87$.

Recently, Allia *et al.* have introduced the so-called reduced magnetoresistance, in order to compare the deviation from the quadratic law of the experimental data obtained from different samples.¹⁰ The reduced magnetoresistance (here called MR_r) varies between zero (for complete saturation) and one (for a demagnetized sample). Defined in terms of Eq. (20), the reduced GMR is simply given by $MR_r = 1/f(1 + MR_n)$. The deviation from the reduced parabola $1 - (M/M_s)^2$ close to $M/M_s = 0$ is larger for larger values of the parameter f which is a measure of the curve flatness [see Fig. 1(b)].

We emphasize that, due to the upper limit of f , a flatness larger than $\langle \mu^{-1/3} \rangle \langle \mu \rangle / \langle \mu^{2/3} \rangle$ cannot be attributed only to the distribution of magnetic moments. Such a large deviation is sometimes observed, as will be discussed in Sec. IV.

D. Distribution function

In order to clarify the above developed ideas, let us now consider a boxlike particle volume distribution function $f(v)$ or, according to Eq. (6), an equivalent magnetic moment distribution function $f(\mu) = N / \ln(\mu_2/\mu_1) \mu$ defined between μ_1 and μ_2 . For this distribution, the magnetization and saturation magnetization given by Eqs. (1) and (3) have an exact solution,^{18,19} namely,

$$M = N \frac{kT}{H} \frac{\ln(x_1 \sinh x_2 / x_2 \sinh x_1)}{\ln(x_2/x_1)}$$

$$\text{and } M_s = N \frac{kT}{H} \frac{x_2 - x_1}{\ln(x_2/x_1)}, \quad (23)$$

where $x_i = \mu_i H / kT$ ($i = 1, 2$).

Unfortunately, there is not such a simple solution for the magnetoresistance given by Eq. (8), and we shall do the integration numerically. Figure 1(a) shows the MR_n vs M/M_s curves calculated with a boxlike distribution function, and Fig. 1(b) shows the corresponding MR_r vs M/M_s curves calculated with the same distribution function. The solid line represents calculations performed with the exact equations (8) and (23). The dotted line (a) and the dashed line (b) were, respectively, drawn in the lower and upper limits of the magnetic field using Eq. (20), and the inverted square parabola (c) was drawn for comparison. The approximate curves fit on the calculated data when $M/M_s < 0.35$ [curve (a)] and $M/M_s > 0.95$ [curve (b)].

We would like to call attention to a detail: Although MR_n and MR_r are equivalent forms to represent the magnetoresistance, the angle between curves (b) and (c) at the limit of high fields is larger in Fig. 1(a) than in Fig. 1(b). In other words, the nonparabolic behavior of the magnetoresistance curve at high fields is more clearly seen in the normalized plot than in the reduced plot.

For practical applications, a log-normal particle volume distribution function $f(v)$ is often assumed. Hence, to conform with Eq. (6), we adopt the following magnetic moment distribution function:

$$f(\mu) = \frac{N}{\sqrt{2\pi}\sigma} \frac{1}{\mu} \exp\left[-\frac{\ln^2(\mu/\mu_0)}{2\sigma^2}\right], \quad (24)$$

which differs from a log-normal distribution function by the factor $1/\mu$.

According to the definition of $\langle \mu^q \rangle$ given by Eq. (11), we have $\langle \mu^q \rangle = \mu_0^q e^{q^2 \sigma^2 / 2}$; in particular, $\langle \mu \rangle = \mu_0 e^{\sigma^2 / 2}$. Consequently, we obtain the following expressions for the parameters f and g :

$$f = \frac{1 + \alpha \mu_0^{-1/3} e^{1/18 \sigma^2}}{1 + \alpha \mu_0^{-1/3} e^{-5/18 \sigma^2}}, \quad g = \frac{1 + \alpha \mu_0^{-1/3} e^{-11/18 \sigma^2}}{1 + \alpha \mu_0^{-1/3} e^{-5/18 \sigma^2}}. \quad (25)$$

Besides, according to Eq. (22), we can easily show that $1 \leq f \leq e^{1/3 \sigma^2}$ and $e^{-1/3 \sigma^2} \leq g \leq 1$.

In the next section, we will fit the magnetization and magnetoresistance curves on experimental data using the distribution function given by Eq. (24). The parameters μ_0 and σ will be determined by fitting the magnetization curve and the parameter α , by fitting the magnetoresistance curve.

III. TEST OF THE THEORETICAL MODEL

The theoretical model developed in the previous section is tested by fitting Eqs. (1) and (8) on experimental data obtained from melt-spun $\text{Cu}_{90}\text{Co}_{10}$ alloys. Continuous ribbons of $\text{Cu}_{90}\text{Co}_{10}$ were obtained by planar flow casting in a He atmosphere on a CuZr wheel and then were submitted to dc

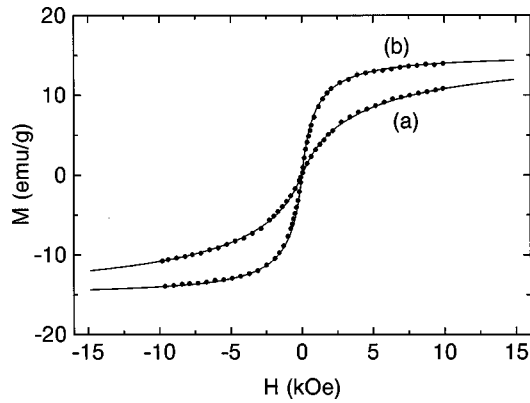


FIG. 2. Magnetization curves for $\text{Cu}_{90}\text{Co}_{10}$ samples annealed by Joule heating under a current I during 60 s. (a) $I=6$ A, fit parameters: $\mu_0=500\mu_B$ and $\sigma=1.16$. (b) $I=6.5$ A, fit parameters: $\mu_0=3900\mu_B$ and $\sigma=0.93$.

Joule heating in a vacuum to induce the precipitation of Co grains. Magnetization and magnetoresistance curves were obtained at room temperature. Magnetoresistance was measured by means of the conventional four-contact technique in the transverse configuration, with the magnetic field applied in the plane of ribbons, perpendicular to the bias current, up to $H=\pm 20$ kOe. Magnetization curves were measured using a vibrating-sample magnetometer (VSM) (LDJ, model 9500), with the applied field varying between ± 10 kOe (see details in Ref. 10). It is important to stress that they have used a unique measurement method to explore the anisotropic magnetization and magnetoresistance curves.²⁰ In this way, it was possible to exclude the small hysteresis present in all samples, retaining only the superparamagnetic contribution.

Figure 2 shows the experimental anhysteretic magnetization data obtained on two samples after annealing by dc Joule heating with electric currents of $I=6$ A (sample *a*) and $I=6.5$ A (sample *b*) during 60 s. The fitting is shown by the solid lines calculated using Eq. (1) with the magnetic moment distribution function given by Eq. (24). As shown in curve (a), good agreement between experimental data and calculations is achieved for the sample annealed under $I=6$ A with the parameters $\mu_0=500\mu_B$ and $\sigma=1.16$. For the sample annealed under $I=6.5$ A, the best fitting is achieved with the parameters $\mu_0=3900\mu_B$ and $\sigma=0.93$ as shown in curve (b). The mean magnetic moments are $\langle\mu\rangle_a=980\mu_B$ and $\langle\mu\rangle_b=6010\mu_B$, which correspond to the mean particle radii $r_a=1.15$ nm and $r_b=2.1$ nm, respectively, if $I_s=1450$ emu/cm³ is assumed for bulk fcc Co.¹⁷ These results are in good agreement with data on granular $\text{Cu}_{90}\text{Co}_{10}$ found in the literature.^{17,20,21} Using Eq. (3), we can calculate from the extrapolated values of the specific saturation magnetization the particle specific densities $N_a=1.7\times 10^{18}/\text{g}$ and $N_b=2.7\times 10^{17}/\text{g}$.

Figures 3(a) and 3(b) show the magnetic moment distribution functions for the two cases described above. Notice the large difference in the abscissa scales, clearly indicating that as a rule particles in sample *b* are much bigger than particles in sample *a*. As a consequence, the magnetization and the magnetoresistance tend to saturation for lower magnetic fields in sample *b* than in sample *a*.

The anhysteretic magnetoresistance data measured on the

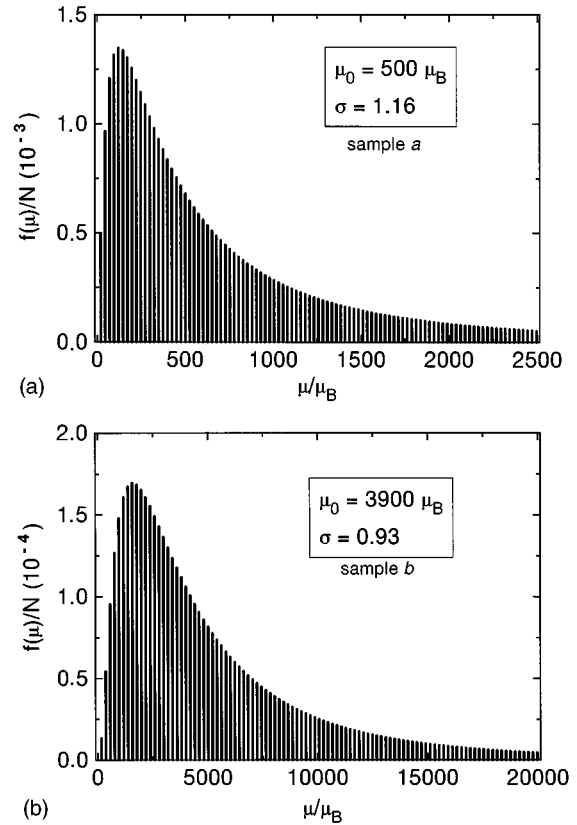


FIG. 3. Magnetic moment distribution functions used to fit the magnetization curves in Fig. 2. (a) $\mu_0=500\mu_B$ and $\sigma=1.16$, (b) $\mu_0=3900\mu_B$ and $\sigma=0.93$.

same samples are shown in Fig. 4, together with the corresponding best fitting curves obtained through Eq. (8) by numerical integration. In order to perform the fitting, we used the distribution function given by Eq. (24) with exactly the same parameters obtained from the fitting of the magnetization curves and just determined the values of the parameter α , which resulted in being $\alpha=110\mu_B^{1/3}$ for curve (a) and $\alpha=80\mu_B^{1/3}$ for curve (b).

It is interesting to note that the pure number $\alpha\mu_0^{-1/3}$ appearing in Eq. (25) is equal to 13.9 for sample *a* and 5.1 for sample *b*. This is the expected behavior, indeed, because,

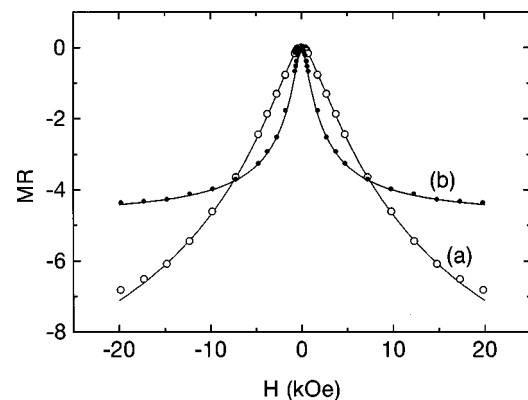


FIG. 4. Magnetoresistance curves for the same samples as in Fig. 2. (a) $I=6$ A, fit parameters: $\mu_0=500\mu_B$, $\sigma=1.16$, and $\alpha=110\mu_B^{1/3}$. (b) $I=6.5$ A, fit parameters: $\mu_0=3900\mu_B$, $\sigma=0.93$, and $\alpha=80\mu_B^{1/3}$.

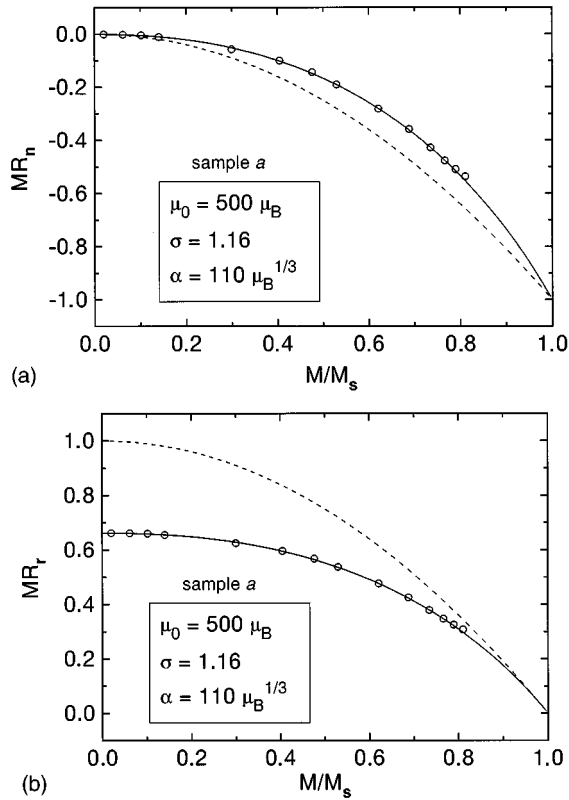


FIG. 5. (a) Normalized MR_n vs M/M_s curve for the sample annealed by Joule heating under an electric current of 6 A during 60 s. Characteristic parameters: $f=1.51$ and $g=0.67$. The square parabola was drawn for comparison (dashed line). (b) Corresponding reduced MR_r vs M/M_s curve.

according to Eq. (9), the parameter $\alpha\mu_0^{-1/3}$ is inversely proportional to the particle radius. Presently, we are performing systematic studies on Cu-Co samples in order to confirm this interesting trend.

Figure 5(a) shows the normalized magnetoresistance MR_n data plotted as a function of the relative magnetization M/M_s for sample *a* (circles). The solid line corresponds to the best fitting obtained through Eqs. (1) and (8) by numerical integration using the distribution function of Fig. 3(a). The normalized parabola that is expected for equal superparamagnetic particles is drawn for comparison (dashed line). In Fig. 5(b), we show the corresponding reduced MR_r vs M/M_s curves. A large flatness is observed around $M/M_s=0$ and a large deviation from the initial quadratic tendency is observed at the saturation point $M/M_s=1$. The flatness parameters $f=1.51$ and $g=0.67$, calculated through Eq. (25), effectively satisfy the conditions given by Eq. (22), since $1 < f < 1.56$ and $0.64 < g < 1$.

The MR_n vs M/M_s and MR_r vs M/M_s curves for sample *b* are shown in Figs. 6(a) and 6(b), respectively. As before, the flatness parameters $f=1.27$ and $g=0.80$ are calculated by means of Eq. (25) and satisfy the conditions expressed by Eq. (22), since $1 < f < 1.33$ and $0.75 < g < 1$.

These results are in good agreement with early observations of Xiao *et al.*^{2,4} revealing a deviation from the quadratic law at high fields.

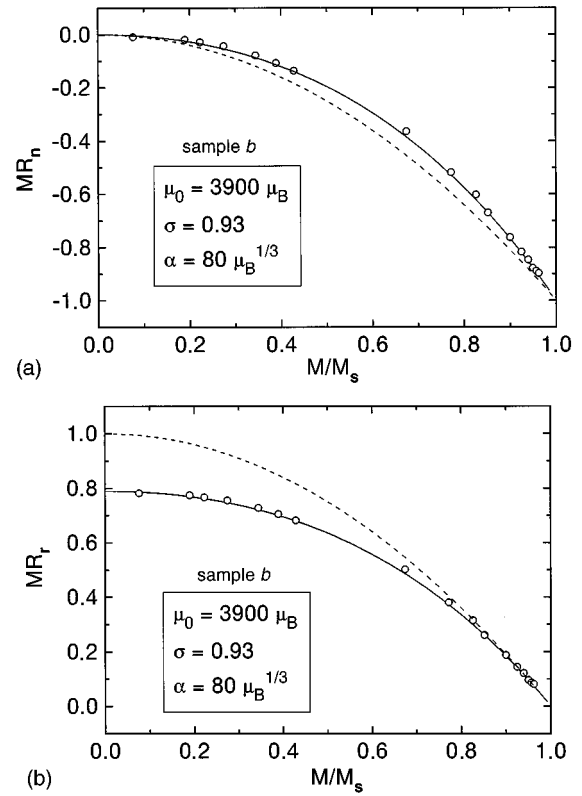


FIG. 6. (a) Normalized MR_n vs M/M_s curve for the sample annealed by Joule heating under an electric current of 6.5 A during 60 s. Characteristic parameters: $f=1.27$ and $g=0.80$. The square parabola was drawn for comparison (dashed line). (b) Corresponding reduced MR_r vs M/M_s curve.

IV. DISCUSSION

The agreement of the model with the experimental results as expressed in the previous section supports the theory of Zhang and Levy about the predominance of boundary scattering over scattering within the grains and settles the need for always taking into account the particle distribution. Notwithstanding, the experimental evidence is not sufficient to establish the parameter α dependence on the mean magnetic moment.

Let us now consider the model in contrast to an alternative explanation of GMR in granular solids found in the literature. Assuming that the model proposed by Gittleman *et al.*³ is valid when there are no interactions between magnetic particles, the deviation from the quadratic behavior observed at low fields is attributed to the particle interactions and the independent behavior described by the parabolic law at high fields is attributed to the high-external-field dominance over the particle interactions. The reduced GMR is plotted against M/M_s in such a way that MR_r must behave as the reduced parabola $1 - (M/M_s)^2$ in the absence of interactions and, otherwise, MR_r must flatten down close to $M/M_s=0$ due to magnetic moment correlations arising from local fields experienced by the interacting particles (see Ref. 10).

Some experimental results are in fact explained by the existence of correlations between magnetic moments, and the presence of strong magnetic interactions is confirmed by

numerous experimental techniques.^{21–25} Furthermore, theoretical calculations demonstrate that interactions have a large influence on the GMR response in granular systems.^{8,10,26}

Hence, both models, one considering particle interactions and the other considering magnetic moment distributions, may describe the observed flatness of the reduced GMR. However, experiments do not give further support to the outlined interaction model. In fact, if the quadratic behavior were manifested at high fields, the flatness would be independent of the MR_r adjustment to the reduced square parabola close to $M/M_s=1$. It has been experimentally observed, however, that the resultant flatness is more pronounced when the achieved magnetization is larger (for larger available magnetic fields), and hence the dependence of GMR on the relative magnetization at high fields is not quadratic.²⁵ This result is clearly in agreement with the magnetic moment distribution model.

In spite of the lack of general validity of the quadratic law at high fields, the assumption about the existence of correlations between interacting magnetic moments at low fields is not disproved by experience. On the contrary, the developed model strongly suggests that interactions may be crucial to explain the flatness of the GMR curve when the conditions expressed by Eq. (22) are not satisfied. As a matter of fact, we applied successfully Eq. (1) to the magnetization data measured on a $\text{Cu}_{90}\text{Co}_{10}$ sample annealed by dc Joule heating under an electric current of 12 A during 4 s and obtained the fitting parameters $\mu_0=4100\mu_B$ and $\sigma=0.915$, with the distribution function given by Eq. (24). Therefore, this magnetic moment distribution function is almost equal to the distribution function of Fig. 3(b). However, we failed in our attempt to fit Eq. (8), since the flatness of the observed magnetoresistance curve $f=2.58$ was far beyond the upper theoretical limit of $e^{\sigma^2/3}=1.32$. From the value of M_s determined by extrapolation, we calculated the particle density $N=8.6\times 10^{17}/\text{g}$ using Eq. (3). Hence, the concentration of magnetic grains in this sample is 3.2 times larger than the concentration in sample *b* annealed under $I=6.5$ A, and correspondingly the mean distance between particles is approximately 1/3 shorter. Beyond any doubt, shorter distances contribute to strengthen magnetic interactions.

Recently, Wisner developed a phenomenological theory of GMR in granular systems according to which the relative magnetoresistance varies almost linearly with the magnetization due to correlations between superparamagnetic and blocked particles.²⁷ In our model, all grains are supposed superparamagnetic (either because they are above the blocking temperature or because the effect of blocked grains is excluded by the measuring technique), but even so we predict a large deviation from the quadratic dependence. As a matter of fact, the magnetization curves of granular systems

display a small hysteresis which may be attributed to blocked particles even at room temperature or to strong interactions between the magnetic grains. The granular structure is extremely complex, indeed, with coexistence of superparamagnetic and ferromagnetic particles interacting among them. We believe that complete understanding of GMR in granular solids will be achieved only when all these factors will be taken into account.

V. CONCLUSION

A simple theoretical model that takes explicitly into account the general distribution of magnetic moments was introduced in order to explain the nonparabolic behavior of the magnetoresistance as a function of the magnetization in granular systems. The model also considers two different electronic scattering mechanisms, one within the magnetic grains and the other at the interface between the grains and the nonmagnetic matrix, from which it is possible to extract valuable information about the origin of the dominant scattering events. Introducing a log-normal-type distribution function, it was possible to test the theoretical model in $\text{Cu}_{90}\text{Co}_{10}$ samples with different grain size distributions. The results indicate that, for the studied samples, the distribution of magnetic moments may explain the noncompliance with the square law of the magnetoresistance as a function of the magnetization as expected for an assembly of equal superparamagnetic particles. Furthermore, the fitting parameters of the model give relevant hints about the involved physics behind the giant magnetoresistance phenomenon, including information about the structure of the granular systems and the basic scattering mechanisms that occur at the boundaries and within the grains. However, it is important to notice that not all experimental data may be explained using the presented model, because it has inherent limits. In some cases, strong magnetic interactions appear, and they must be introduced in the model. Systematic studies of samples with continuously growing grain sizes that are currently being performed will allow us to confirm the ideas expressed in this paper and to introduce the effect of magnetic interactions upon the dependence of GMR on magnetization.

ACKNOWLEDGMENTS

The authors are greatly indebted to Dr. Franco Vinai and Dr. Paola Tiberto, from the Istituto Elettrotecnico Nazionale Galileo Ferraris (Torino, Italy), for making the anhysteretic measurements available to us. We also gratefully acknowledge elucidative discussions with Dr. Paolo Allia (Torino, Italy) and Dr. Cristina Gómez Polo (Pamplona, Spain). This work was supported by local (FAEP/UNICAMP), state (FAPESP), and federal (CAPES) Brazilian agencies.

¹A. E. Berkowitz, J. R. Mitchell, M. J. Carey, A. P. Young, S. Zhang, F. E. Spada, F. T. Parker, A. Hutten, and G. Thomas, Phys. Rev. Lett. **68**, 3745 (1992).

²J. Q. Xiao, J. S. Jiang, and C. L. Chien, Phys. Rev. Lett. **68**, 3749 (1992).

³J. I. Gittleman, Y. Goldstein, and S. Bozowski, Phys. Rev. B **5**, 3609 (1972).

⁴J. Q. Xiao, J. S. Jiang, and C. L. Chien, Phys. Rev. B **46**, 9266 (1992).

⁵J. F. Gregg, S. M. Thompson, S. J. Dawson, K. Ounadjela, C. R.

- Staddon, J. Hamman, C. Fermon, G. Saux, and K. O'Grady, *Phys. Rev. B* **49**, 1064 (1994).
- ⁶S. Zhang and P. M. Levy, *J. Appl. Phys.* **73**, 5315 (1993).
- ⁷Ju. H. Kim, J. Q. Xiao, C. L. Chien, Z. Tesanovic, and L. Xing, *Solid State Commun.* **89**, 157 (1994).
- ⁸M. El-Hilo, K. O'Grady, and R. W. Chantrell, *J. Appl. Phys.* **76**, 6811 (1994).
- ⁹B. J. Hickey, M. A. Howson, S. O. Musa, and N. Wisser, *Phys. Rev. B* **51**, 667 (1995).
- ¹⁰P. Allia, M. Knobel, P. Tiberto, and F. Vinai, *Phys. Rev. B* **52**, 15398 (1995).
- ¹¹R. Y. Gu, L. Sheng, D. Y. Xing, Z. D. Wang, and J. M. Dong, *Phys. Rev. B* **53**, 11685 (1996).
- ¹²A. Vedyayev, B. Mevel, N. Ryzhanova, M. Tshiev, B. Dieny, A. Chamberod, and F. Brouers, *J. Magn. Magn. Mater.* **164**, 91 (1996).
- ¹³C. Bellouard, B. George, and G. Marchal, *J. Phys.: Condens. Matter* **6**, 7239 (1994).
- ¹⁴C. L. Chien, J. Q. Xiao, and J. S. Jiang, *J. Appl. Phys.* **73**, 5309 (1993).
- ¹⁵A. E. Berkowitz, J. R. Mitchell, M. J. Carey, A. P. Young, D. Rao, A. Starr, S. Zhang, F. E. Spada, F. T. Parker, A. Hutten, and G. Thomas, *J. Appl. Phys.* **73**, 5320 (1993).
- ¹⁶T. A. Rabedeau, M. F. Toney, R. F. Marks, S. S. P. Parkin, R. F. C. Farrow, and G. R. Harp, *Phys. Rev. B* **48**, 16810 (1993).
- ¹⁷R. von Helmolt, J. Wecker, and K. Samwer, *Phys. Status Solidi B* **182**, K25 (1994).
- ¹⁸E. Kneller, *Z. Phys.* **152**, 574 (1958).
- ¹⁹H. G. Zolla and F. Spaepen, *Mater. Sci. Eng. A* **204**, 71 (1995).
- ²⁰P. Allia, F. Ghigo, M. Knobel, P. Tiberto, and F. Vinai, *J. Magn. Magn. Mater.* **157/158**, 319 (1996).
- ²¹R. H. Yu, X. X. Zhang, J. Tejada, J. Zhu, M. Knobel, P. Tiberto, P. Allia, and F. Vinai, *J. Appl. Phys.* **78**, 5062 (1995).
- ²²T. Sugawara, K. Takanashi, K. Hono, and H. Fujimori, *J. Magn. Magn. Mater.* **159**, 95 (1996).
- ²³A. Gavrin, M. H. Kelley, J. Q. Xiao, and C. L. Chien, *Appl. Phys. Lett.* **66**, 1683 (1995).
- ²⁴X. Battle, V. Franco, A. Labarta, M. L. Watson, and K. O'Grady, *Appl. Phys. Lett.* **70**, 132 (1997).
- ²⁵A. D. C. Viegas, J. Geshev, L. S. Dorneles, J. E. Schmidt, and M. Knobel, *J. Appl. Phys.* (to be published).
- ²⁶P. Vargas, D. Altbir, J. d'Albuquerque e Castro, and U. Raff (unpublished).
- ²⁷N. Wisser, *J. Magn. Magn. Mater.* **159**, 119 (1996).